Temperature cycles in the Heisenberg spin glass

L. Berthier*

*Laboratoire des Colloïdes, Verres et Nanomatériaux, Université Montpellier II and UMR 5587 CNRS,
34095 Montpellier Cedex 5, France*

A. P. Young[†]

Department of Physics, University of California, Santa Cruz, California 95064, USA

We study numerically the nonequilibrium dynamics of the three-dimensional Heisenberg Edwards-Anderson spin glass submitted to protocols during which temperature is shifted or cycled within the spin glass phase. We show that (partial) rejuvenation and (perfect) memory effects can be numerically observed and study both effects in detail. We quantitatively characterize their dependences on parameters such as the amplitude of the temperature changes, the time scale at which the changes are performed, and the cooling rates used to vary the temperature. We contrast our results both to those found numerically in the Ising version of the model, and to experimental results in different samples. We discuss the theoretical interpretations of our findings, arguing, in particular, that "full" rejuvenation can be observed in experiments even if temperature chaos is absent.

I. INTRODUCTION TO BASIC PHENOMENA

In recent work[1] we studied the nonequilibrium dynamics of the Heisenberg Edwards-Anderson spin glass model in three dimensions following a sudden quench to its low-temperature phase. Here we continue our investigations of the nonequilibrium, low-temperature dynamics of this model by analyzing its behavior in more complex protocols, similar to those performed in experiments.[2–4] More precisely, we consider in detail the effects of a temperature cycle (illustrated in Fig. 1) consisting of the following three steps:

• Quench the system from $T=\infty$ to a temperature T_1 at time $t_w=0$, and wait a time t_1.

• Then change the temperature to a lower value T_2 and wait a further time t_2.

• At total time $t_w=t_1+t_2$ change the temperature back to T_1.

This temperature cycling protocol has been used extensively to characterize several spin glass systems,[2–15] and these studies motivated similar cycling experiments on many different types of glassy materials.[16–25]

Numerical studies of temperature shifts and cycles in the Ising version of the model have been reported,[26–33] and temperature cycles have been discussed theoretically.[34–42] However, the Heisenberg spin glass model has been much less studied than its Ising counterpart, even though it is closer to many of the experimentally studied spin glass systems, and only a few aging studies exist.[1,32,43,44] In particular, extensive studies of temperature cycles have not been reported (see Ref. 32 for preliminary results) and we attempt here to fill this gap.

The Heisenberg spin glass model that we study has the Hamiltonian

$$H = -\sum_{\langle i,j \rangle} J_{ij}\mathbf{S}_i \cdot \mathbf{S}_j, \tag{1}$$

where the sum is over nearest neighbors of a cubic lattice of linear size $L=60$ with periodic boundary conditions, the $\mathbf{S}_i$

are three-component vectors of unit length and coupling constants are drawn from a symmetric Gaussian distribution of standard deviation unity. We refer to our previous paper[1] for the technical details concerning our simulations. When performing temperature cycles a large number of parameters can be varied, implying a larger numerical effort than was needed in the simple aging studies of Ref. 1.

The basic quantity we measure is the two-time autocorrelation function of the spins, $C(t_w,t_w+\tau)$, defined by
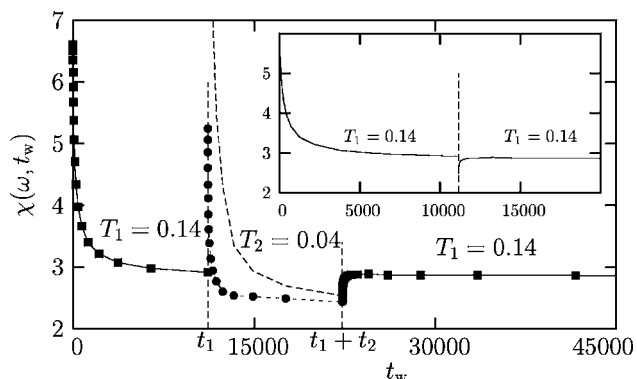

FIG. 1. Time evolution of $\chi(\omega,t_w)$ in a temperature cycle performed with the three-dimensional Heisenberg spin glass for $1/\omega=1078$. Aging is observed in the first $t_1=11\,159$ sweeps during which the temperature is at $T_1=0.14 < T_c \simeq 0.16$. The temperature is then quenched to $T_2=0.04$ for the next $t_2=11\,159$ sweeps. This causes aging to restart, a rejuvenation effect. The long-dashed line shows the result of a direct quench from $T=\infty$ to T_2 at time t_1. The variation of $\chi(\omega,t_w)$ with t_w is much stronger than when the temperature is shifted from T_1 to T_2, showing that rejuvenation in the temperature shift is only partial. At $t_w=t_1+t_2$ the temperature is shifted back to its initial value, and the data seems to be simply a continuation of that for $t_w < t_1$. This memory effect is illustrated more clearly in the inset where the intermediate time spent at $T_2=0.04$ has been removed.

214429-1

$$C(t_w, t_w + \tau) = \frac{1}{L^3} \sum_i \langle \mathbf{S}_i(t_w) \cdot \mathbf{S}_i(t_w + \tau) \rangle, \tag{2}$$

where the brackets indicate an average over both disorder and thermal fluctuations. The latter is performed by repeating the simulation for different initial conditions. To compare with experiment we often plot instead

$$\chi(\omega, t_w) \equiv \frac{1 - C(t_w, t_w + \omega^{-1})}{T}, \tag{3}$$

since this is expected to have similar behavior to the ac magnetic susceptibility at frequency ω.

A representative sample of our results for a temperature cycle is shown in Fig. 1. For $t_w < t_1$ this is just a "simple aging" experiment corresponding to quenching the system infinitely fast from an infinite to a low temperature, $T_1 = 0.14 < T_c \simeq 0.16$. Physical quantities then slowly relax toward equilibrium, which is known as aging. We have characterized this behavior in detail in Ref. 1.

For $t_1 < t_w < t_1 + t_2$, during which the temperature is $T_2 = 0.04 < T_1$, the signal just after the shift is not a simple continuation of the decay at the previous temperature. The system has apparently forgotten it is already "old" and it seems therefore "rejuvenated" by the temperature change. In experiments performed on Heisenberg spin glasses, when $T_1 - T_2$ is sufficiently large, the signal obtained after the shift can be exactly superposed on the one obtained after a direct quench from $T = \infty$ to $T = T_2$, implying that the system behaves as if it had fully forgotten the time spent at temperature T_1. We will call this situation "full rejuvenation." However, rejuvenation is not full in our simulations because the change in $\chi(\omega, t_w)$ with time during the part of the temperature cycle at T_2 is less than the change found in a direct quench to T_2, which is shown by the long-dashed line in Fig. 1. Since we do not observe full rejuvenation we will need to ask whether the observed behavior is rejuvenation at all or whether it can be fully explained in terms of the cumulative aging scenario, discussed below in Sec. II. We will also investigate the possible origins of this significant difference between numerical and experimental results, and will discuss in particular the role of finite cooling rates in experiments in Secs. III C and V C.

Finally, in the third part of the experiment, $t_w > t_1 + t_2$, the relaxation proceeds, after a short transient, as if the second step had not occurred. The system has kept a "memory" of the first aging step, despite the strong restart observed in the second part of the protocol. In the inset of Fig. 1, we show that the third part of the experiment appears to be the simple continuation of the first part, as if the second step had not taken place, which we call a "perfect memory effect." This figure is not entirely convincing, though, because the signal is nearly flat and small deviations from perfect memory could be invisible on that scale. That memory is indeed close to perfect, at least for large temperature shifts, will be more quantitatively demonstrated in Sec. IV.

In the rest of this work, we analyze in more detail the rejuvenation and memory effects seen in Fig. 1. In Sec. II we give some theoretical background on the cumulative aging scenario, according to which the effects seen are simply due to changes in the rate of growth of correlations with temperature. Our data on rejuvenation and memory are described in Secs. III and IV, respectively. We discuss our results in Sec. V, and give a final summary in Sec. VI.

II. CUMULATIVE AGING

An important theoretical concept in understanding nonequilibrium data for spin glasses is that of a dynamical correlation length, $\xi(T, t)$, which describes the spatial extent of spin correlations after aging a time t at temperature T. In the cumulative aging scenario, it is proposed that the observed phenomena can be understood solely in terms of the time and temperature dependences of $\xi(T, t)$. We now discuss the predictions of cumulative aging, first for the step down in temperature from T_1 to T_2, which can lead to rejuvenation, and then for the subsequent step back up to T_1, which can lead to memory.

A. Cumulative aging and rejuvenation

If the correlation length grows to a value $\xi(T_1, t_1)$ by waiting a time t_1 at T_1, then one would have to wait a longer time, $t_{\text{eff}}^{\text{cum}}$, at the lower temperature T_2 to get the same correlation length, where this "effective age" in the cumulative aging scenario is given by

$$\xi(T_1, t_1) = \xi(T_2, t_{\text{eff}}^{\text{cum}}). \tag{4}$$

If the growth law $\xi(T, t)$ is known accurately, Eq. (4) can be used to determine $t_{\text{eff}}^{\text{cum}}$ for given values of T_1, T_2, and t_1.

In practice one can try to fit the data for $\chi(\omega, t_1 + t)$ during the time spent at T_2 to data for $\chi_{T_2}(\omega, t_{\text{eff}} + t)$, i.e., data in a single quench to T_2 for some waiting time $t_{\text{eff}} + t$ with t_{eff} used as a free fitting parameter. In other words t_{eff} is determined from matching both sides of the following equation:

$$\chi(\omega, t_1 + t) = \chi_{T_2}(\omega, t_{\text{eff}} + t). \tag{5}$$

One of the following scenarios might then occur. A first possibility is that

$$t_{\text{eff}} = 0, \tag{6}$$

which corresponds to full rejuvenation. The time spent at T_1 is irrelevant for aging at T_2. This is seen experimentally for large temperature shifts, but not in any of our simulations.

Second, one might find that

$$t_{\text{eff}} = t_{\text{eff}}^{\text{cum}}, \tag{7}$$

where $t_{\text{eff}}^{\text{cum}}$ is given by Eq. (4). This is the so-called cumulative aging scenario. We shall see in Sec. IV B that this case describes our simulations when the temperature difference $T_1 - T_2$ is small, though we show in Sec. III A that it does not work when $T_1 - T_2$ is large. However, Eq. (7) does not correspond to rejuvenation. Rather, rejuvenation is defined to be the additional effect beyond Eq. (7), since the latter simply reflects the change in the rate of growth of the correlation length with temperature.

A third possibility is that

$$0 < t_{\text{eff}} < t_{\text{eff}}^{\text{cum}}. \tag{8}$$

This is one way in which partial rejuvenation could occur, and is seen in some experiments[6,7,12] at intermediate values of the temperature shift. However our simulations do not fit this scenario. Rather, for large values of $T_1 - T_2$ we will see in Sec. III A that our data cannot be collapsed onto data for a direct quench by shifting the time. Hence the effective age t_{eff} cannot be defined in our simulations at large temperature differences, and so our results in this region do not fit any of the above scenarios.

Remark that if t_1 and $T_1 - T_2$ are sufficiently large, $t_{\text{eff}}^{\text{cum}}$ will be much larger than t_1. One can make this statement more quantitative by assuming, as usual, that equilibration proceeds by activation over barriers, where the barrier height ΔE is some function of the length scale ξ. Writing $t = t_0 \exp(\Delta E(\xi)/T)$, where t_0 is a microscopic attempt time that we set to 1, Eq. (4) gives

$$T_1 \ln t_1 = T_2 \ln t_{\text{eff}}^{\text{cum}}, \tag{9}$$

which can be written as

$$\ln\left(\frac{t_{\text{eff}}^{\text{cum}}}{t_1}\right) = \left(\frac{T_1 - T_2}{T_2}\right) \ln t_1. \tag{10}$$

Hence if $(T_1 - T_2) \ln t_1 > T_2$, we have $t_{\text{eff}}^{\text{cum}} \gg t_1$. As a result, $\chi(\omega, t_1 + t)$, given by Eq. (5), will vary very little with t unless t greatly exceeds t_1, which is not the case in the simulations. Although the reasoning leading to Eqs. (9) and (10) is for a particular simple model of the growth of the correlation length, we expect the result $t_{\text{eff}}^{\text{cum}} \gg t_1$ to be more generally correct.

B. Cumulative aging and memory

In a similar way we can fit the data for $\chi(\omega, t_1 + t_2 + t)$ after the step back up to T_1 to data for $\chi_{T_1}(\omega, t_1 + t_{\text{eff}} + t)$,

$$\chi(t_1 + t_2 + t) = \chi_{T_1}(\omega, t_1 + t_{\text{eff}} + t), \tag{11}$$

assuming that the two functions of t in this expression can be matched for a particular choice of t_{eff}. If memory is perfect then

$$t_{\text{eff}} = 0, \tag{12}$$

so that the time spent at T_2 simply plays no role in the subsequent aging at T_1.

In the cumulative aging scenario $t_{\text{eff}} = t_{\text{eff}}^{\text{cum}}$, where

$$\xi(T_1, t_1 + t_{\text{eff}}^{\text{cum}}) = \xi(T_2, t' + t_2), \tag{13}$$

in which t' is the time the system would have to age at T_2 to get the correlation length it reached at T_1 after time t_1. It is given implicitly by

$$\xi(T_2, t') = \xi(T_1, t_1), \tag{14}$$

as in Eq. (4) above. This is shown graphically for a set of experimental parameters in Fig. 12, later.

It is worth mentioning that at extremely long times or for very large changes in temperature one expects perfect memory, even in the cumulative aging scenario. This is be-
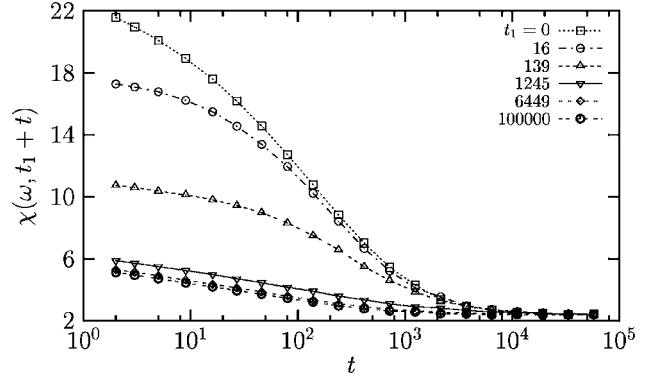

FIG. 2. The behavior of $\chi(\omega, t_1 + t)$ during the time t spent at temperature $T_2 = 0.04$ for different values of the time, t_1, waited at $T_1 = 0.14$. We fix $1/\omega = 1078$. For $t_1 = 0$, the system undergoes a direct quench to $T = T_2$, while for $t_1 \to \infty$, the system has time to equilibrate at T_1. The restart of aging (rejuvenation) is reduced when t_1 increases from 0, but remains nonzero even when $t_1 \to \infty$.

cause, at long times, the growth of ξ with time at the lower temperature T_2 is much slower than at T_1, so t' is huge, the difference $\xi(T_2, t' + t_2) - \xi(T_2, t')$ is small, and hence $t_{\text{eff}}^{\text{cum}}$ is small. As in Sec. II A, we can make this more quantitative within a barrier activation model for which Eqs. (13) and (14) imply

$$T_2 \ln(t' + t_2) = T_1 \ln(t_1 + t_{\text{eff}}^{\text{cum}}), \tag{15}$$

$$T_2 \ln t' = T_1 \ln t_1. \tag{16}$$

We expect perfect memory if

$$t' \gg t_2 \quad (\text{perfect memory}). \tag{17}$$

Since $t_1 \sim t_2$, from Eq. (16) this gives

$$\frac{T_1 - T_2}{T_2} \gg \frac{1}{\ln t_1} \quad (\text{perfect memory}). \tag{18}$$

Equation (17) is equivalent to the condition $t_{\text{eff}}^{\text{cum}} \ll t_2$ since the elimination of t' from Eqs. (15) and (16) gives

$$\frac{t_{\text{eff}}^{\text{cum}}}{t_2} = \frac{T_2}{T_1} \exp\left[-\left(\frac{T_1 - T_2}{T_2}\right) \ln t_1\right], \tag{19}$$

assuming $t_{\text{eff}}^{\text{cum}} \ll t_1$. Hence, if Eq. (18) is satisfied, one has perfect memory in the cumulative aging scenario. This conclusion should again be more general than the particular barrier activation model we used.

III. REJUVENATION

Now we discuss in detail our results for the behavior following the temperature drop to T_2 and their interpretation.

A. Do we really observe rejuvenation?

It is clear from Fig. 1 that aging is strongly restarted when temperature changes from $T_1 = 0.14$ to $T_2 = 0.04$, but that, unlike in experiments, the effect is weaker than when the system is directly quenched to T_2. In Fig. 2 we show the sys-
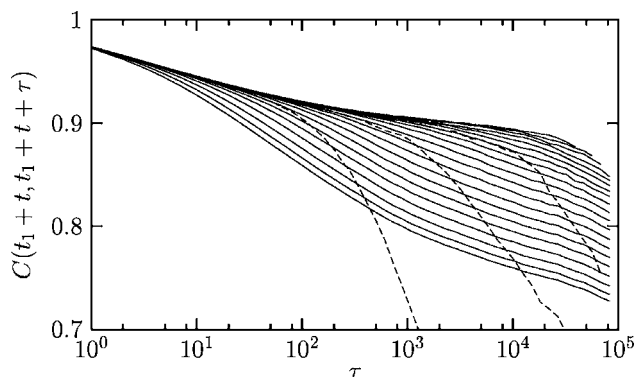
FIG. 3. The full lines show data for the two-time spin autocorrelation function $C(t_1+t,t_1+t+\tau)$ as a function of the time difference τ. The time spent at $T_1=0.14$ is $t_1=10^5$ and the different curves are for different values of t, the time waited at $T_2=0.04$, increasing from $t=2$ (the lowest) to $t=57\,797$ in a logarithmic progression. This data shows that aging is restarted in a temperature shift. The dashed lines are the autocorrelation function measured in a direct quench to $T_2=0.04$ and waiting times $t=416$, 3728, and $19\,307$ (from left to right). A comparison shows that the shape of the data found in reducing the temperature from T_1 to T_2 is different from that in the direct quench to T_2.

tematic trend in the data when we vary the time t_1 spent at the upper temperature T_1. Two important pieces of information can be deduced from Fig. 2.

• The case of $t_1=0$ corresponds to a direct quench from $T=\infty$ to $T=T_2$. We see from Fig. 2 that the signal obtained after waiting for a finite value of t_1 at $T=T_1$ is different from the signal obtained in a direct quench and differs more as t_1 is increased. In "full rejuvenation," as seen in experiments, the data after waiting a time t_1 is the same as in a direct quench. We were not able to vary parameters of temperature cycles in such a way that full rejuvenation is observed in our simulations.

• When t_1 increases, the signal saturates to a limiting behavior. This is actually the region in which the intermediate part of Fig. 1 was obtained, since t_1 is quite large there. This saturation implies that even if we were able to equilibrate the system at temperature T_1, it would undergo aging when further quenched to T_2. This is very different from the behavior of a pure ferromagnet, for instance, which would reequilibrate on a microscopic time scale upon a similar temperature change within its ferromagnetic phase.

We have therefore seen that rejuvenation is not full. We will now argue that it is not null either and that there is an additional signal beyond that expected in the cumulative aging scenario discussed in Sec. II. To do so it is useful to look at the dependence of $\chi(\omega,t_1+t)$ on frequency, or equivalently the dependence of the two-time autocorrelation function on the time difference τ. The solid lines in Fig. 3 show data for this quantity. The system has spent a large time $t_1=10^5$ at $T=T_1=0.14$, sufficiently large that the data in Fig. 3 has become independent of t_1. The different curves are for different values of t, the time waited at $T_2=0.04$, increasing from $t=2$ to $57\,797$ in a logarithmic progression. The curves do not superpose and the behavior observed in Fig. 3 is qualitatively similar to that obtained in simple aging experiments, where

samples undergo a rapid quench to the spin glass phase. There is a first, fast stationary decay of the autocorrelation functions followed by a second, much slower, age-dependent decay. However, there is a quantitative difference since the precise shape of the data is actually not the same as in a direct quench to T_2. The difference can be appreciated in Fig. 3 by comparing the solid with the dashed lines, which are for a direct quench with various waiting times. In the direct quench, the correlation function decays faster at long time differences.

For the temperature shift to T_2 in Fig. 1, we have seen in Fig. 3 that the shape of the extra signal due to this shift is different from the result of a direct quench to T_2. We also need to ask whether the magnitude of the extra signal is greater than that expected in the cumulative aging scenario discussed in Sec. II.

In Fig. 1, the time $t_1=11\,159$ is large, since the data in Fig. 2 has saturated for this value of t_1, and the temperature shift T_1-T_2 is large. Hence, as discussed in Sec. II A, the effective age in the cumulative aging scenario is enormous, and the time dependence of χ should be tiny in this scenario. This is clearly not the case for the data in Fig. 1. We conclude that for large temperature shifts there is genuine rejuvenation; the cumulative aging scenario does not work. In addition, the fact that the data of Fig. 3 is independent of t_1, at large t_1, for all $\tau\equiv\omega^{-1}$, implies that the above conclusion on the existence of rejuvenation holds for any frequency ω accessible in our simulations.

We note that the use of a different "clock" to determine effective ages could lead to the wrong impression that we observe full (or close to full) rejuvenation.[7,30,45] If one follows a common experimental procedure and defines $t_{\rm eff}$ as the location of a peak in the logarithmic derivative of the two-time autocorrelation function, $S(t,t+\tau)=\partial C(t,t+\tau)/\partial\log\tau$, one obtains a very small effective age from the data of Fig. 3 and then conclude that rejuvenation is almost full. We know, however, for example by comparing the shapes of the solid and dashed curves in Fig. 3, that this is not the case. Hence $S(t,t+\tau)$ cannot be used to quantify rejuvenation in numerical simulations of temperature shifts. This remark was already made for the Ising spin glass in Ref. 30, although in a less detailed way.

Data for a range of temperature shifts is presented in Fig. 4. We see that the amplitude of the restart of aging is strongly dependent on the amplitude of the temperature shift. The case where $T_2=T_1$ has no restart of aging and corresponds to a simple quench to T_2 (with the plot starting at waiting time t_1). For $T_2<T_1$ there is an additional decay of $\chi(\omega,t)$ due to the temperature shift. We shall see in Sec. IV B that this effect is describable by cumulative aging for small temperature shifts, unlike the situation for large temperature shifts discussed earlier in this section.

As a final comment, we note that the restart of aging observed in the second part of the cycle shown in Fig. 1 is not an artifact produced by our choice of $\chi(\omega,t)$ as a physical observable, as suggested in Refs. 32 and 33. It is certainly true that the susceptibility, defined by Eq. (3) and the correlation function are not related by a fluctuation-dissipation relation since the system is not in equilibrium,
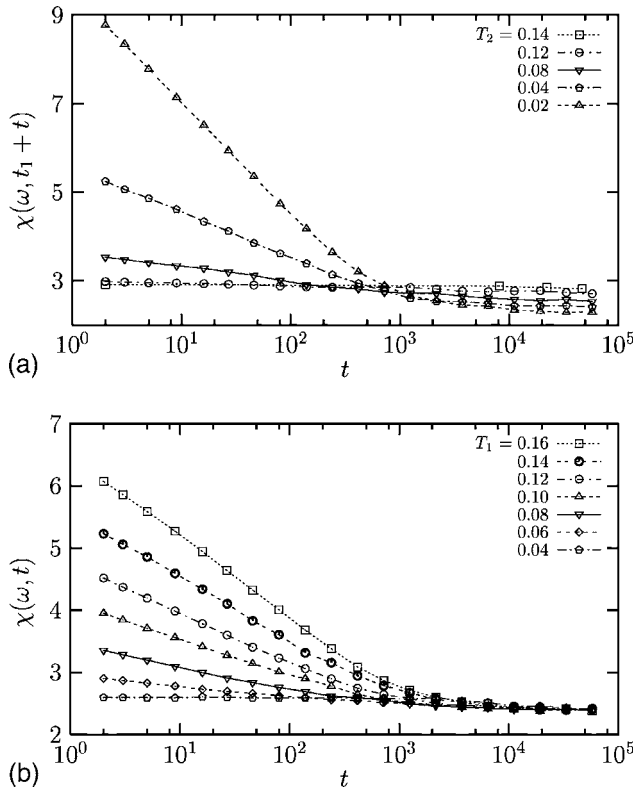
FIG. 4. Top: Changing the second temperature. The protocol is $T=\infty \rightarrow T_1=0.14$ at time 0. Temperature is kept constant for $t_1 =11\,159$ sweeps after which it is shifted to various $T_2 \leqslant 0.14$. Bottom: Changing the first temperature. The protocol and notations are as above but with a fixed $T_2=0.04$ and different $T_1 \geqslant T_2$. In both figures the additional amplitude of the aging signal increases with T_1-T_2. While cumulative aging works for small values of T_1-T_2, see Sec. IV, there is a genuine additional rejuvenation signal at large temperature differences.

and so rejuvenation effects might appear to be stronger using one or the other observable. However, Fig. 3 leaves us with no doubt concerning the fact that aging is restarted in a shift.

B. Is temperature chaos relevant?

In this section we discuss our results about rejuvenation effects from a theoretical point of view. As already mentioned, the growth of correlations with time is characterized by a dynamical correlation length $\xi(T,t)$. Length scales that are active at T_1 in a given time window t, $\xi_1 \equiv \xi(T_1,t)$, are typically larger than the ones active at $T_2 < T_1$ in the same time window, $\xi_2 \equiv \xi(T_2,t) < \xi_1$. Although $\xi(T,t)$ is only a gradual function of T at fixed time t, ξ grows very slowly (presumably logarithmically) with t and so it can take an astronomical amount of time to relax excitations of size ξ_1 at the lower temperature T_2. Roughly speaking, changing the temperature gives only a modest change in length scales but a huge change in time scales. For practical purposes, excitations of size ξ_1 are frozen at T_2 and dynamics at T_2 is due to fluctuations at the smaller length scale ξ_2, which had easily reached quasiequilibrium at temperature T_1. Rejuvenation therefore means that equilibrium states at T_1 and T_2 are sig-

nificantly "different" on length scales of the order of ξ_2. What "different" really means will be the subject of this subsection.

Theoretically two explicit examples of this difference have been discussed in the literature:

• Temperature chaos in the scaling picture of spin glasses.[34,47–50]

• Temperature dependence of the exponent of the power-law decay of spatial correlations in the two-dimensional non-disordered XY model.[39]

In the temperature chaos scenario, spin orientations are spatially uncorrelated beyond an overlap length, $\ell_o(T_1-T_2)$, which diverges when $T_1-T_2 \rightarrow 0$ but is small at large temperature differences, $\ell_o \sim |T_1-T_2|^{-1/\zeta}$, where ζ is an exponent quantifying chaos. Chaos can therefore naturally explain full rejuvenation if $\ell_o < \xi_2$ because equilibrium states at the two temperatures are uncorrelated at the important length scale of ξ_2. As a consequence, aging at T_1 is unable to bring the system closer to equilibrium at T_2. In the opposite situation, $\ell_o > \xi_2$, called "weak chaos," a smaller but nonzero rejuvenation signal should be observed,[7] since there are some rare regions of space, occurring with probability $(\xi_2/\ell_o)^\zeta$, which are affected by the temperature change.

In the two-dimensional nondisordered XY model below its Kosterlitz-Thouless transition temperature T_{KT}, equilibrium spin correlations decay with a power of the distance r, $C(\mathbf{r}) \sim r^{-\eta(T)}$, where the exponent $\eta(T)$ depends continuously on T. This is because there is a line of critical points for $0 < T \leqslant T_{KT}$. Hence, when temperature is changed from T_1 to T_2 all length scales have to readjust to the new critical point,[51] whatever the time spent at T_1. Interestingly, this produces a rejuvenation signal that is not full but becomes gradually larger when T_1-T_2 is increased.[39]

We now investigate which of these two scenarios corresponds most closely to our simulations. In Ref. 1 we showed that spatial spin glass correlations at short distances, $r < \xi(T,t)$, are well described by algebraic decays with a temperature-dependent exponent,

$$C_4(\mathbf{r},t) \sim r^{-\alpha(T)} \quad (r < \xi(T,t)) \quad (20)$$

[where C_4 is defined in Eq. (21) below], just as in the two-dimensional XY model. Moreover, the rejuvenation effect we observe in the present study has the same characteristics as the one found in the XY model, since it is never full but becomes gradually larger when T_1-T_2 is increased. As for the Ising spin glass model[29] this shows that the rejuvenation signal observed in simulations is largely due the temperature dependence of spatial correlations via the exponent $\alpha(T)$.

It remains to ask, though, whether there are additional rejuvenation effects observed in our simulations due to temperature chaos. In Refs. 29 and 30, it was argued that the answer for three- and four-dimensional Ising spin glasses is "no." The reason is that chaotic effects with temperature are very hard to detect, presumably because the overlap length is never small in Ising systems.[48,49] However, equilibrium calculations for vector spins suggest that overlap lengths should be smaller in the Heisenberg case,[50] while dynamic length scales are larger than in the Ising model.[1] Hence it appears potentially easier to detect chaotic temperature effects in
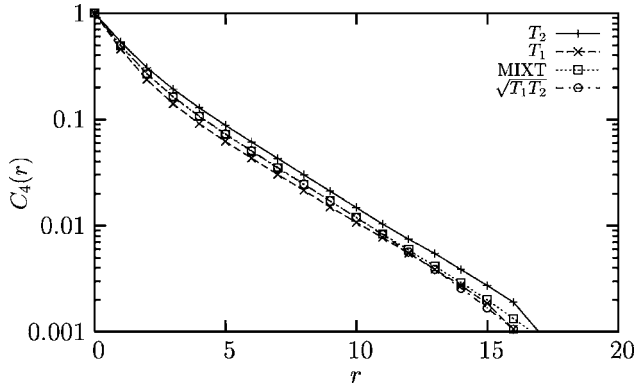
FIG. 5. Spatial correlations between two replicas, a and b, at equal temperatures $T_1 = 0.14$ ("T_1") and $T_2 = 0.04$ ("T_2"), or different temperatures ("MIXT"). The curve noted "$\sqrt{T_1 T_2}$" is the square root of the product of the data at T_1 and T_2 and coincides with the "MIXT" points, as expected in the absence of chaos.

FIG. 6. Effect of a noninfinite initial temperature in a quench. The system is first quenched from $T = \infty$ to various temperatures, $T_i > T_c \simeq 0.16$. Temperature is kept constant at T_i during 10^4 time steps after which it is quenched to the final temperature $T_1 = 0.04$ at time $t_w = 0$.

Heisenberg systems than in Ising systems,[44] so this possibility needs to be investigated.

To do so we follow Ref. 29 and consider a two-site, two-replica correlation function,

$$C_4(\mathbf{r}, t) = \frac{1}{L^3} \sum_i \langle \mathbf{S}_i^a(t) \cdot \mathbf{S}_{i+\mathbf{r}}^a(t) \mathbf{S}_i^b(t) \cdot \mathbf{S}_{i+\mathbf{r}}^b(t) \rangle, \qquad (21)$$

where the two replicas a and b have the same interactions but age independently at different temperatures, T^a and T^b, with $\Delta T \equiv T^a - T^b$. If $\ell_o(\Delta T) < \xi(T^a, t)$ then the overlap between the spin configurations in the two replicas becomes small in a simulation on time scale t.

In Fig. 5 we show our results for the Heisenberg model with the same two temperatures $T_1 = 0.14$ and $T_2 = 0.04$ used in our previous cycles. Data is presented for the two-replica correlators in three different cases.

- $T^a = T^b = T_1$, and $t_w^a = t_w^b = 3728 = t_1$, noted "$T_1$."
- $T^a = T^b = T_2$, and $t_w^a = t_w^b = 57797 = t_2$, noted "$T_2$."
- $T^a = T_1$, $T^b = T_2$, $t_w^a = 3728$, and $t_w^b = 57797$, noted "MIXT."

The simulation times have been chosen so that $\xi(T_1, t_1) \simeq \xi(T_2, t_2)$. This equality can be seen in Fig. 5 because the correlation functions "T_1" and "T_2" are parallel in this log-lin representation at large r. By contrast these curves have a different slope at small r because short distance behavior is characterized by the temperature-dependent exponent $\alpha(T)$ in Eq. (20).

Since the temperatures T_1 and T_2 are very different, we need to take into account the overall increase of spin glass order as the temperature is lowered.[40] We therefore also plot $\sqrt{C_4(r, T_1, t_1) C_4(r, T_2, t_2)}$, which is called "$\sqrt{T_1 T_2}$" in Fig. 5. We find that "MIXT" and "$\sqrt{T_1 T_2}$" are equal within our numerical precision, the result expected in the absence of chaos. We conclude that even weak chaotic effects are not detectable in our numerical simulations despite large temperature jumps, $\Delta T / T_c \sim 0.625$, and large dynamic length scales; see the range for r in Fig. 5. The dynamic rejuvenation effects we observe can therefore be attributed entirely to the temperature dependence of the exponent $\alpha(T)$ in Eq. (20)
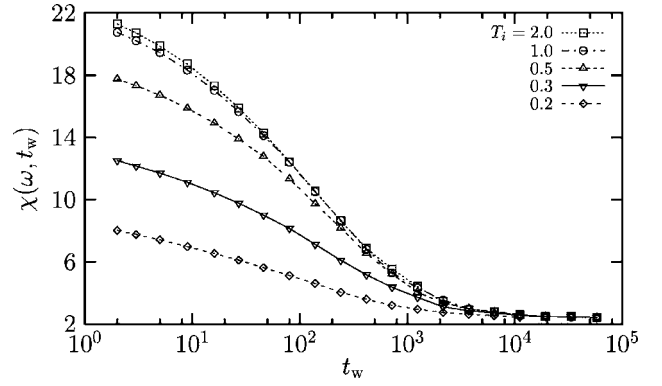
describing the power law decay of spatial correlations at distances less than $\xi(T, t)$.

Of course temperature chaos could still exist at larger length scales. Although the time scales of experiments (relative to the microscopic time) are much longer than in simulations, the difference in length scales is not so pronounced, as we shall emphasize in Sec. V. Hence, we feel it is unlikely that strong temperature chaos occurs in experiment either. Unfortunately, this is difficult to check since direct probes of length scales related to chaos effects are not experimentally feasible. As discussed in detail in Sec. V C, the experimental observation of full rejuvenation does not in itself prove that a strongly chaotic situation is reached in experiments.

C. What is a direct quench in experiments?

To our knowledge, full rejuvenation has never been found in numerical studies even in large temperature shifts, in contrast to experiments that do find full rejuvenation. One difference in procedures is that temperature changes in simulations are instantaneous, whereas they can only take place at a finite rate in experiments. We therefore need to study whether correlations built up during gradual cooling are relevant to the subsequent dynamics. If chaos were important in the simulations, the answer would presumably be no, since the growth of correlations with time has to restart from scratch at each temperature. However, as we showed in Sec. III B, no chaos effects are seen in our simulations. Hence we need to consider the effects of gradual changes in temperature, to see whether these modified protocols improve agreement with experiment.

First, rather than quenching from $T = \infty$ to T_1, we consider the effect of taking a finite initial temperature, $T_c < T_i < \infty$. This protocol allows us to investigate the effect of building spatial correlations at high temperatures on the aging dynamics at lower temperature. Our results for various T_i are presented in Fig. 6, where we have adopted the following procedure. The temperature is quenched from $T = \infty$ to T_i where it is kept constant for 10^4 sweeps after which the temperature is instantaneously quenched to the final temperature $T_1 = 0.04$.

For initial temperatures larger than $T_i \simeq 2.0 \simeq 12.5 T_c$ the aging observed at $T_1 = 0.04$ is similar to the one observed in a quench from $T_i = \infty$. However, as soon as $T_i < 2.0$ aging is affected. In particular, the total amplitude of the relaxation,

$$\Delta \chi(\omega) = \chi(\omega, t = 0) - \chi(\omega, t = \infty), \qquad (22)$$

is greatly reduced when T_i decreases. We then use Eq. (22) to compare the aging dynamics in various protocols. From Fig. 2 we find that the ratio of the amplitude of relaxation in a truly direct quench to the amplitude in a $0.14 \rightarrow 0.04$ shift is about 5 while full rejuvenation would imply that this ratio is 1. If, however, one compares the $0.14 \rightarrow 0.04$ shift to a direct quench from a finite temperature, say from $T_i = 0.3 \simeq 1.9 T_c$, to $T = 0.04$, this ratio becomes $\simeq 2.8$, i.e. closer to the full rejuvenation result. We conclude that spending some time at high temperatures makes the rejuvenation signal closer to what is observed experimentally, though we still do not see full rejuvenation.

In real experiments, not only is the initial temperature finite, as above, but also the cooling from T_i to T_1 is not instantaneous. Therefore not only does the system build correlations at high temperature T_i, but it also has some dynamics at all temperatures intermediate between T_i and T_1. This is likely to influence even more the aging dynamics at the final temperature.

To investigate this point we have performed simulations of temperature cycles using finite cooling rates. We repeated the temperature cycles of Sec. I using a realistic protocol. The system is first quenched from $T = \infty$ to $T_i = 2.0$, where it is kept constant during 10^4 sweeps. Then the temperature is decreased at a finite cooling rate, R, so that the time evolution of the temperature is of the form $T(t) = T_i - Rt$. The cooling is stopped at $T_1 = 0.14$ for a time t_1, after which the temperature is decreased to $T_2 = 0.04$ at the same cooling rate R. We simulated cycles with two different cooling rates, $R_1 = 0.002$ and $R_2 = 0.0005 = R_1/4$ [cooling rates are expressed in units of J/t_0, where $J = 1$ is the variance of the distribution of coupling constants in Eq. (1) and $t_0 = 1$ is the Monte Carlo time unit]. These values were chosen to give cooling times comparable to $1/\omega$, as in experiments.[14] We find that a finite cooling rate has two effects:

• All the amplitudes of relaxation are reduced. This is a somewhat natural observation.

• A less trivial result is that ratio of amplitudes between a direct quench to T_2 and a shift through T_1 are again reduced from their $R = \infty$ values. When $1/\omega = 1078$, we find that these ratio are 5, 3.8, and 3 for $R = \infty$, R_1 and R_2, respectively.

These results again indicate that the finite cooling rates used in experiments make the observed rejuvenation effects closer to that in experiments, though we are still far from full rejuvenation. In fact, we shall argue in Sec. V C that full rejuvenation is expected in experiments because of the much larger range of time scales that are probed there than in the simulations.

We have shown that a nonideal quench very strongly affects aging behavior. In fact we find that all scaling behaviors reported in Ref. 1 for simple aging experiments are affected. This is a likely explanation of the "subaging" behavior systematically found in experiments[2,14] while simulations indi-
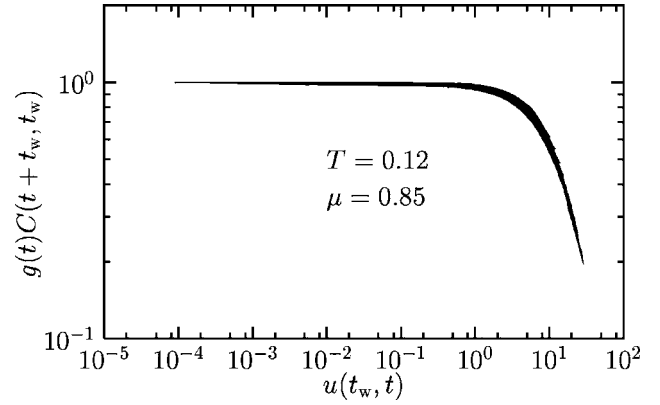

FIG. 7. Subaging behavior found at $T = 0.12$ when the initial temperature is $T_i = 0.3$ and the cooling rate infinite. The horizontal axis is $u(t_w, t) = [(t + t_w)^{1-\mu} - t_w^{1-\mu}]/(1-\mu)$ which reduces to t/t_w when $\mu = 1$, and the vertical axis involves a factor $g(t)$ to account for quasiequilibrium short-time behavior; see Ref. 1 for details. The parameter μ is adjusted to get the best data collapse for different values of t_w. The case $\mu < 1$, as found here, corresponds to subaging. The case, $\mu = 1$, which we find when the initial temperature is $T = \infty$, corresponds to simple aging.

cate instead "superaging" behavior.[1,29] As a single example we show in Fig. 7 the effect of a noninfinite initial temperature, $T_i = 0.3$, on the aging at temperature $T = 0.12$. The cooling rate is infinite. When $T_i = \infty$ a simple scaling of correlation functions is observed at this temperature,[1] $C(t_w, t + t_w) \sim g^{-1}(t) \mathcal{C}(t/t_w)$, where $g(t)$ accounts for the short-time quasiequilibrium behavior. Instead, when $T_i = 0.3$, we find that a more complicated, subaging scaling form is needed, as shown in Fig. 7. We have systematically found subaging behavior in nonideal quenches. Given that experimental cooling times are always extremely large when compared to microscopic time scales, it is not surprising that this effect persists experimentally,[14] unless specific but empirically determined protocols are used.[46] Cooling rate effects also imply that aging dynamics probed (a) numerically, and (b) experimentally in "direct quenches," are fundamentally different, which prevents a quantitative comparison of their scaling behavior.

IV. MEMORY

Memory effects are simpler to understand than rejuvenation effects. They directly result from the strong influence of temperature on the time scales needed to equilibrate fluctuations on a given length scale. Dynamics at different temperatures but in similar time windows probe different length scales.[4,29,34,36,37,42] In this section we quantify these effects.

A. Is there perfect memory for large shifts?

In the inset of Fig. 1 we have shown that the aging in the third step of the temperature cycle appears to be, after a short transient, the perfect continuation of the first step. However, this data is not completely convincing because $\chi(\omega, t_w)$ decreases very slowly on the time scale of the simulation. It is better to study the full frequency dependence, or, equiva-
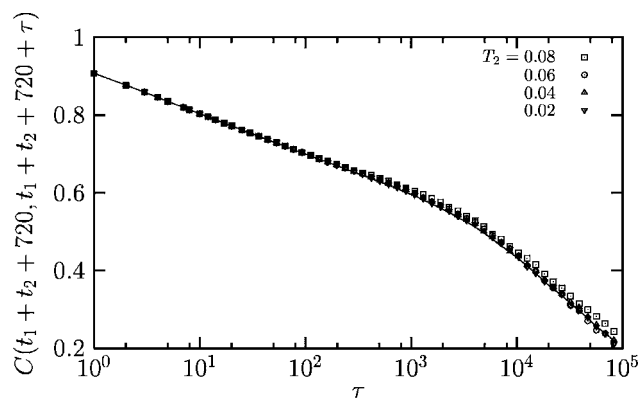
FIG. 8. Time decay of the autocorrelation function $C(t_1+t_2+720, t_1+t_2+720+\tau)$ in the third step of temperature cycles with perfect memory. The protocol is as in Fig. 1, i.e. $T_1=0.14$, $T_2=0.04$, $t_1=t_2=11\,159$. The waiting time $t_w=t_1+t_2+720$ corresponds roughly to the end of the transient seen in Fig. 1. The full line is the autocorrelation measured in a direct quench to $T_1=0.14$ after waiting $t_1=11\,159$, i.e. $C_{T_1}(t_1,t_1+\tau)$. If memory is perfect, the data from the cycle agrees with that from the direct quench. Small deviations from perfect memory are visible at $T_2=0.08$, but absent for lower T_2 for which "memory's perfect."

FIG. 10. The effective age $t_{\rm eff}$ in a shift experiment for different values of T_1 at fixed t_2. The system is quenched at $T_2=T_1-\Delta T$, where it ages during a time $t_2=11\,159$, after which the temperature is shifted up to various temperatures T_1. Open symbols are for the Heisenberg spin glass, filled symbols for the Ising spin glass. The solid line marked "activation" is the prediction from cumulative aging assuming barrier activation, Eq. (24). The line marked "modified activation" is also for the cumulative aging scenario, but assuming a different form for $\xi(T,t)$, namely $\xi(T,t)\sim t^{1/z(T)}$ with $z(T)=(T_0/T)^{0.85}$, which fits growth laws for the Ising spin glass.

lently, the time dependence of the spin autocorrelation function.[29]

In Fig. 8 we show that the memory effect observed in Sec. I is indeed convincing, or, in an allusion to Billy Wilder, that "memory's perfect."[52] The decay of the autocorrelation function in the third stage of the cycle for large T_1-T_2 is indeed the same, within our numerical accuracy, as the one obtained if the second stage of the experiment is dropped out. As in experiments, we conclude that despite the strong rejuvenation effect observed in the second stage at temperature T_2, the correlations built in the first stage at temperature T_1 have been perfectly preserved and can be retrieved when temperature is shifted back to its initial value.

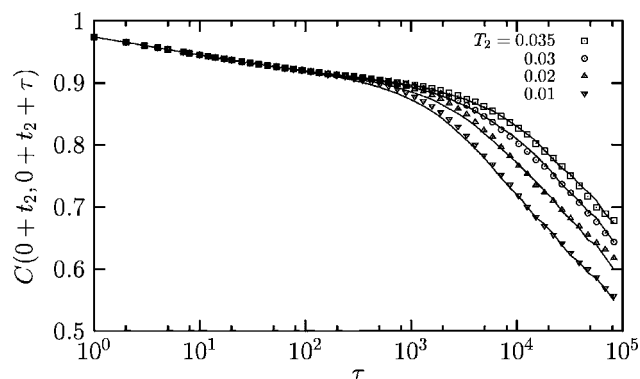FIG. 9. Influence of the aging at low temperature $T_2<0.04$ on the subsequent aging at $T_1=0.04$. The system is quenched directly from $T=\infty$ to T_2 (so $t_1=0$), where it is kept during $t_2=11\,159$ time steps, after which the temperature is shifted up to $T_1=0.04$. Autocorrelation functions in these shifts are shown with symbols. They are compared to the ones, shown with full lines, measured in a direct quench to $T_1=0.04$ and different waiting times $t_w=2700$, 4500, 7000 and 9500 (from left to right), chosen to match the temperature shift data. The matching is seen to work well.
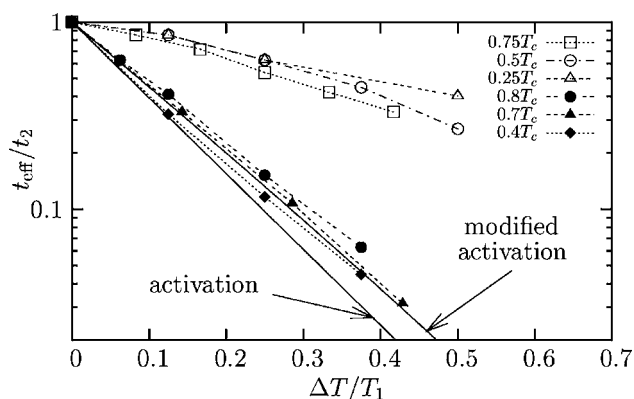
B. Is there memory for small shifts?

In the previous section we showed that memory is essentially perfect for large temperature shifts. We now discuss what happens for smaller values of the temperature shift where we will see that cumulative aging becomes a good approximation. To compare with the cumulative aging scenario we extract an effective age $t_{\rm eff}$ by fitting the data for $\chi(\omega,t_1+t_2+t)$ to Eq. (11). Ideally one can find a $t_{\rm eff}$ value so that this data is equal to $\chi_{T_1}(\omega,t_1+t_{\rm eff}+t)$ for all t. For technical reasons it is difficult to measure the effective age when times get large because the change in χ becomes too small. Hence we will extract $t_{\rm eff}$ using a protocol with $t_1=0$, i.e. a sudden quench to $T=T_2$ followed by an upward shift to $T=T_1$ at time t_2. This modified protocol does not correspond to the cycle discussed in Sec. I but is used here as a convenient mean to measure effective aging times. Also, we will actually do the fit to the time-dependent correlation function in Eq. (3). This is, of course, equivalent to fitting data for χ.

Figure 9 shows some data for this protocol as a function of $\tau=\omega^{-1}$ with $T_1=0.04$, $t_1=t=0$, and $t_2=11\,159$. Just after the shift up to T_1 we record the time decay of the spin autocorrelation functions. By definition, when $T_2=T_1$ the autocorrelation function follows the curve obtained in a direct quench to $T_1=0.04$ after $t_w=11\,159$. However, when $T_2<T_1$ the time decay of the autocorrelation function after the shift becomes faster, but an effective age, $t_{\rm eff}<t_w$, can still be defined, since the solid lines in Fig. 9, which are from direct quenches, go through the points, which are from the temperature shift protocol. In other words, matching the correlation functions as a function of $\tau=\omega^{-1}$ to the expression analogous to Eq. (11) with $t_1=t=0$ works well. We see from Fig. 9 that $t_{\rm eff}$ progressively decreases when T_2 decreases, as expected in the cumulative aging scenario of Sec. II. Physically this means that aging at low temperature is less effec-
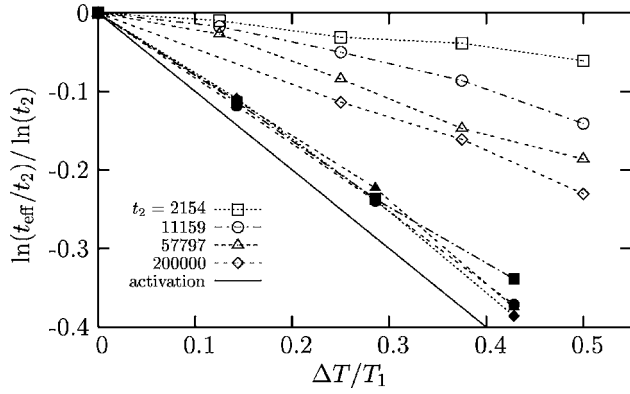
FIG. 11. Effective ages in shift experiments for different values of t_2 at fixed T_1. The system is quenched at $T_1 - \Delta T$, where it ages during a time t_2. The temperature is then shifted up to T_1. Open symbols are for the Heisenberg spin glass with $T_1 = 0.08 \approx 0.5 T_c$, filled symbols for the Ising spin glass with $T_1 = 0.7 T_c$, but the same times t_2 as the Heisenberg model. The straight line is the prediction of cumulative aging with thermal activation, Eq. (24).

tive at building spatial correlations, or, in other words, that the growth of the dynamic correlation length is slower at a lower temperature.

We have repeated this matching procedure for many different shifts, changing t_2 from 2154 to 2×10^5 time steps, the final temperature from $T_1 = 0.4$ to $T_1 = 0.12$, and the amplitudes of the shift, $\Delta T = T_1 - T_2$, from $\Delta T = 0.01$ to $\Delta T = 0.05$. The results are presented in Figs. 10 and 11, which also contain similar data for the Ising spin glass that are discussed below in Sec. IV C.

We now compare our results for t_{eff} to the prediction of the cumulative aging scenario

$$\xi(T_1, t_{\text{eff}}^{\text{cum}}) = \xi(T_2, t_2), \qquad (23)$$

which is just Eq. (13) with $t_1 = t' = 0$. For each of the parameters T_1, T_2, and t_2 corresponding to the points for the Heisenberg model in Fig. 10, we determined $t_{\text{eff}}^{\text{cum}}$ using Eq. (23) and data for $\xi(T, t)$ in Ref. 1. The ratios of $t_{\text{eff}}^{\text{cum}}$ to t_{eff} determined from fits like those in Fig. 9 are presented in Table I. We see that the ratio roughly takes values in the range $\left[\frac{1}{2}, 2\right]$, with no obvious systematic behavior. That the ratio is not perfectly 1 is hardly surprising given that one has

to make use twice of imperfect numerical data to estimate $t_{\text{eff}}^{\text{cum}}$ from Eq. (23). We conclude, contrary to the preliminary investigations of Ref. 32, that the cumulative aging hypothesis, Eq. (23), is a good interpretation of the behavior of the Heisenberg spin glass in temperature shifts of small amplitude. Quite importantly, these results validate the assumption of cumulative aging used in Refs. 5, 8, and 37, where experimental data plotted as in our Figs. 10 and 11 is one of the ingredients used to reconstruct growth laws for $\xi(T, t)$.

Alternatively, rather than estimate $\xi(T, t)$ from the numerical data of Ref. 1, one can assume an analytical form for the growth law, for example, the barrier activation model used to obtain Eqs. (9), (15), and (16). This predicts

$$\ln\left(\frac{t_{\text{eff}}^{\text{cum}}}{t_2}\right) = -\frac{\Delta T}{T_1} \ln t_2, \qquad (24)$$

which is equivalent to Eq. (9), with the roles of T_1 and T_2 interchanged. It corresponds to the straight solid line marked "activation" in Figs. 10 and 11. We find that for all temperatures the measured t_{eff} lie significantly above this result. Moreover, the dependence upon the final temperature T_1 at fixed t_2 is weak. From the growth laws for $\xi(T, t)$ reported in Ref. 1 this result is reasonable, since the dynamic correlation length is very weakly dependent on temperature for times smaller than $t \sim 10^3$, and only after that does it enter a regime dominated by thermal activation.[1] We therefore expect that shifts performed at larger times t_2 will get closer to the cumulative aging scenario with a barrier activation form for $\xi(T, t)$.

We confirm this expectation in Fig. 11, where we work with a constant final temperature, $T_1 = 0.08 \approx 0.5 T_c$, but change the duration of the initial period over two orders of magnitude. To compare data with different shifting times, we plot $\ln(t_{\text{eff}}/t_2)/\ln t_2$ vs $\Delta T/T_1$ for which cumulative aging with thermal activation, Eq. (24), predicts a linear relation of slope -1, independent of t_2. Upon increasing t_2 we find that the data get closer to this prediction, but still lie systematically above it. Similar results are found for $T_1 = 0.12 \approx 0.75 T_c$. As a rough estimate, if the evolution of these curves persists at much larger times it would require about 4 more orders of magnitude, i.e. $t_2/t_0 \sim 10^9$, to get curves that eventually lie on or below the thermally activated estimate. This is not inconsistent with the experimental finding that

TABLE I. An evaluation of the cumulative aging hypothesis in small temperature shifts.

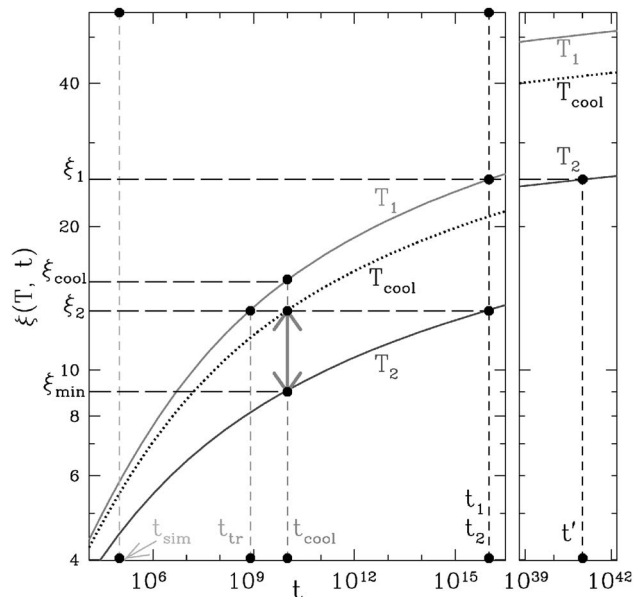| T_2	T_1	t_2	t_{eff}	$t_{\text{eff}}^{\text{cum}}$	$t_{\text{eff}}/t_{\text{eff}}^{\text{cum}}$
0.02	0.04	11 159	4500	4200	1.07
0.04	0.08	11 159	3000	4200	0.71
0.10	0.12	11 159	8000	5500	1.45
0.08	0.12	11 159	4700	3800	1.24
0.04	0.08	2154	1350	1300	1.04
0.04	0.08	57 797	7500	11 000	0.68
0.10	0.12	57 797	29 000	15 000	1.93
0.08	0.12	57 797	13 000	11 500	1.13
0.14	0.12	11 159	22 500	22 000	1.02

FIG. 12. Solid curves show $\xi(T,t)$ (with t in units of the microscopic time $t_0=10^{-12}$ s) inferred in Ref. 37 for a Heisenberg spin glass at temperatures $T_1/T_c=0.825$, and $T_2/T_c=0.7$. Note the break in the horizontal scale between the two boxes. We assume waiting times at T_1 and T_2 of $t_1=t_2=10^4$ s$=10^{16}t_0$. The length scales equilibrated at T_1 and T_2 are $\xi_1 \equiv \xi(T_1,t_1)$ and $\xi_2 \equiv \xi(T_2,t_2)$ (indicated by horizontal long-dashed lines). To reach length scale ξ_1 at the lower temperature T_2 one would have to wait a time $t' \simeq 10^{41}t_0 \simeq 3 \times 10^{21}$ yr, given by Eq. (14). This is truly astronomical, so fluctuations between ξ_2 and ξ_1 are effectively frozen during the time t_2 spent at T_2. This is the origin of the memory effect. When the temperature is raised back to T_1, see Fig. 1, fluctuations on length scale ξ_2 have to reequilibrate at T_1, which takes a "transient" time $t_{tr} \simeq 10^9 = 10^{-3}$ s (which is very short; another requirement for perfect memory). We also show t_{cool}, the time spent "close to" a given temperature during cooling, and indicate, by a dotted line, the growth at $T=T_{cool}=0.795T_c$, the temperature at which $\xi(T_{cool},t_{cool})$ is equal to ξ_2. We also define $\xi_{cool}=\xi(T_1,t_{cool})$. In cooling to $T=T_2$ the system will have correctly equilibrated for temperature T_2 up to scale $\xi_{min}=\xi(T_2,t_{cool})$. During subsequent aging for time t_2 at $T=T_2$, fluctuations on scales between ξ_{min} and ξ_2 (shown by the thick line with arrows) have to reequilibrate, provided correlations on scales less than $\xi(T,t)$ vary with T [for example, by the dependence of the exponent α on T in Eq. (20)]. This gives rise to rejuvenation. The time scale probed in our simulations is of order $t_{sim} \simeq 10^5$, which is much smaller than in experiments. However, the difference between the length scales probed in experiment and simulations is much smaller than the difference in time scales.

these curves lie below the Arrhenius line in Heisenberg spin glass samples[5,8,14] since experiments are performed on time scales that are typically 10^{12}-10^{16} times larger than microscopic flipping times; see, e.g., Fig. 12.

In this section we performed upward temperature shifts of relatively small amplitude. We expect that cumulative aging would also work for small temperature changes in a downward shift, but for technical reasons it is difficult to test extensively this hypothesis directly, because effective ages very quickly become too large to be numerically measurable in downward shifts. We nevertheless add in Table I the result

for a downward $0.14 \rightarrow 0.12$ shift from the data displayed in Fig. 4(a). For this particular example, cumulative aging works indeed very correctly.

C. Does spin anisotropy play a role?

In this section we compare our results for the temperature shifts with similar results obtained in the three-dimensional Ising spin glass, using exactly the same thermal protocols and the same procedure to extract effective ages. To this end we needed to extend significantly the numerical results obtained by one of us and Bouchaud in Ref. 29 to which we refer for technical details concerning the Ising simulations. These new results for the three-dimensional Ising Edwards-Anderson spin glass are reported along the ones for the Heisenberg model in Figs. 10 and 11.

A quantitative comparison between the two sets of data can be performed if one assumes that in both cases, Monte Carlo time units represent the microscopic flipping time which we fix to $t_0=1$ in both simulations—a physically reasonable assumption. From the comparison between the two models one can draw two main conclusions.

• Curves for the Ising spin glass lie below the ones of the Heisenberg model for all the shifts we have performed, so t_{eff}/t_2 is smaller for the Ising case. In other words, the effect of a temperature shift on aging dynamics is stronger for the Ising simulations. However, the opposite behavior is observed in experiments which compare strongly anisotropic (Ising) samples with isotropic (Heisenberg) samples.[8]

• Changing the duration of the shift over two orders of magnitude has a strong effect on the Heisenberg spin glass, as described in Sec. IV B above, but very little or no effect in the Ising case; see Fig. 11. To our knowledge there are no systematic experimental investigations concerning this point but if this trend persists to much larger time scales, it could lead to a situation where Heisenberg data lies below the "activation" curve while Ising data lies above it, as is found experimentally.[8]

The Ising data agrees better with the barrier activation form for $\xi(T,t)$ in the cumulative aging picture than does the Heisenberg data. Although we use the terminology "barrier activation" the same result, Eq. (24), applies if the barrier height only depends logarithmically on length scale, in which case[27,28,32] $\xi(T,t) \sim t^{1/z}$ with $z=T_0/T$, i.e. ξ grows with a power of t. Recently, algebraic laws with $z=(T_0/T)^\gamma$ with $\gamma \simeq 0.85$ were reported.[32] As shown in Fig. 10 the introduction of the adjustable parameter γ allows one to understand deviations from simple thermal activation in the Ising spin glass within the cumulative aging hypothesis. Possibly critical fluctuations near T_c renormalize the microscopic flipping time[5,6,29] in such a way that the growth is approximately of this form in numerical time windows. It would be interesting to check if experimental data taken in anisotropic (Ising) samples can be fitted with the same "modified activation" growth law.

V. DISCUSSION

A. Memory effects

Memory effects stem from thermally activated dynamics which implies that temperature so strongly influences the

growth of the dynamic correlation length, $\xi(T,t)$, that aging is much less effective at building spatial correlations at lower temperatures. Therefore length scales that are quasiequilibrated at some temperature T_1 can effectively be frozen if the temperature is decreased to $T_2 < T_1$. Spatial patterns imprinted in the systems at T_1 are then naturally retrieved when temperature is shifted back to its original value. From this perspective it is natural that memory effects are found in so many different disordered materials where activated dynamics is ubiquitous.[1–25]

In Fig. 12 we show an example of growth laws as extracted from experimental data in Heisenberg samples in Ref. 37. The precise details of the fits that gave these curves will not be relevant here because our main conclusions will be qualitative. We use this graph to discuss a temperature cycle occurring between temperatures $T_1 = 0.825 T_c$ and $T_2 = 0.7 T_c$. With[37] $T_c = 16.7$ K, this gives $T_1 = 13.77$ K and $T_2 = 11.69$ K, so that $\Delta T \simeq 2$ K, as in the original experiment of Ref. 9.

For concreteness we assume a microscopic time of $t_0 = 10^{-12}$ s and take $t_1 = t_2 = 10^4$ s so, in units of the microscopic time, we have $t_1 = t_2 = 10^{16}$. The correlation lengths ξ_1 and ξ_2 reached at T_1 and T_2 in a time $t_1 = t_2$ are 25.3 and 13.3, respectively, indicated by dashed horizontal lines. To reach a length scale of ξ_1 at the lower temperature T_2 would require an astronomically large time of order $t' \simeq 10^{41} t_0 = 10^{29}$ s, given by Eq. (14), which is indicated in the right-hand box of the figure. Also relevant is an estimate of the transient time, t_{tr}, required to reequilibrate fluctuations at scale ξ_2 when the temperature is increased back to T_1. This is given implicitly by $\xi(T_1, t_{tr}) = \xi_2 \equiv \xi(T_2, t_2)$. From Fig. 12 we see that t_{tr} is of order 1 ms, hardly detectable if the frequency is of the order of a few Hz. In general, we expect perfect memory if Eq. (17) and the condition

$$t_{tr} \ll t_2 \quad \text{(needed for perfect memory)}, \qquad (25)$$

are both satisfied. Within the barrier activation model and for $t_1 \sim t_2$, Eqs. (17) and (25) are actually equivalent since this model predicts that

$$\frac{\ln t_2}{\ln t_{tr}} = \frac{\ln t'}{\ln t_1} = \frac{T_1}{T_2}. \qquad (26)$$

Equation (18), which corresponds to Eq. (17) for the barrier activation model, is satisfied for the experimental situation in Fig. 12, so memory should be perfect, as was indeed found.[9] However, Eq. (18) is harder to satisfy in numerical simulations since the time scales are shorter. Hence larger temperature steps have to be chosen in simulations, but, nonetheless, Eq. (18) can then be satisfied. This conclusion holds for both Heisenberg and Ising spin glass models.[26,28,29,31–33]

While the details of the numbers in this discussion can be debated, it is surely true in general that changing the temperature in experiments gives a large change in time scales (though not a very large change in length scales), and that perfect memory can be obtained in this situation with moderate to large temperature shifts.

B. Physical origin of rejuvenation effects

We have seen in Sec. V A that to get memory it is sufficient to have a wide separation of time scales. We now turn to rejuvenation effects that are more difficult to understand since, by itself, Fig. 12 does not explain why aging is strongly restarted when the temperature is shifted from T_1 to T_2. The important question is that, since excitations on length scales active at T_2 were fully equilibrated at T_1 just before the shift, why do they need to reequilibrate at all upon a small temperature change?

In this paper we have been able to answer this question for the Heisenberg spin glass model simulated on time scales up to 10^5. We find that spatial correlations at equilibrium [i.e. at distances less that $\xi(T,t)$] are close to algebraic with a temperature-dependent exponent $\alpha(T)$, see Eq. (20), so that excitations on all length scales up to ξ have to readapt at each temperature. This interpretation is very close to the physical interpretation of the behavior of the two-dimensional XY model when temperature is shifted along its critical line.[39]

As discussed in Sec. III B we found no trace of chaotic behavior of spatial correlations with temperature, though it is possible that chaotic effects could set in at larger length scales. However, in the hypothetical temperature cycle of Fig. 12, which corresponds to experimental parameters, we see that the difference in length scales probed by simulations and experiments is not very drastic (a factor of about 3 or 4) so we are tempted to conclude that chaos also does not occur in experiments. Even if it did, chaotic effects would appear in addition to the signal characterized in this paper, so experimental results would present a mixed character, difficult to analyze quantitatively within one scenario or the other.

The situation found here is qualitatively very similar to what is observed numerically in Ising spin glasses in various dimensions.[26,28–31] Differences between models arise only at a quantitative level. For instance, in the three-dimensional Ising spin glass, the exponent α only depends weakly on temperature taking the value of about 0.5 throughout the spin glass phase.[29] Correlations change more significantly in four dimensions[29] with α changing from 0.9 and 1.6 between $0.5 T_c$ and T_c. As a result, rejuvenation effects are relatively pronounced in four dimensions, while almost absent in three.[28,31] By comparison, α in the three-dimensional Heisenberg spin glass has an intermediate behavior[1] since it changes from 0.8 to 1.1 between $0.5 T_c$ and T_c. However, this relatively small variation is compensated by the fact that dynamic length scales for the Heisenberg model are also larger than for the Ising case.

C. Experimental observation of full rejuvenation

We have seen in Sec. V B that the observation of partial rejuvenation in the simulations for large temperature shifts can be well understood. Here, we give a plausible explanation of the full rejuvenation observed experimentally, an important ingredient being a very large separation of time scales, much larger than is feasible in simulations.

As mentioned in Sec. III C, "direct" quenches in experiment are not instantaneous, and incorporating this into the

simulations gave results which were somewhat closer to full rejuvenation. Here we develop a phenomenological description of aging, which includes a finite cooling rate. An important concept in it is the time spent "close to" a given temperature,[53] where a precise definition of "closeness" will not be needed to illustrate the main points qualitatively, but presumably requires that spatial correlations (on the cooling time scale) do not change "much" while the temperature is "close" to a given value. Let us denote this time scale by t_{cool}. As an example, if we assume that a quench takes place in 1 s, and divide this time into 100 intervals, we have $t_{cool} = 0.01 \text{ s} = 10^{10} t_0$, as indicated in Fig. 12. This is certainly rough, but we can vary t_{cool} quite substantially without invalidating our main conclusions.

It will be convenient, for the subsequent discussion, to define various length and time scales that arise in quenching down to $T = T_2$ at a given rate. Correlations on length scale r will freeze, i.e. drop out of equilibrium, at temperature $T_f(r)$, where

$$\xi(T_f(r), t_{cool}) = r. \qquad (27)$$

To determine the extent of rejuvenation in a T shift to T_2, we need to consider the correlations on length scales up to ξ_2. The temperature where correlations on this scale fall out of equilibrium is

$$T_{cool} = T_f(\xi_2), \qquad (28)$$

which is $T_{cool} \simeq 0.795 T_c$ in the example shown in Fig. 12. During the cooling process, when the temperature has reached $T = T_1$ the correlation length will be

$$\xi_{cool} \equiv \xi(T_1, t_{cool}), \qquad (29)$$

see Fig. 12. When the system has been cooled down to $T = T_2$, the system will be equilibrated for this temperature up to scale,

$$\xi_{min} = \xi(T_2, t_{cool}), \qquad (30)$$

which is also shown in Fig. 12.

We are now in a position to compare aging after a "direct quench" to T_2 with that following a temperature shift from T_1 to T_2. Suppose first that $T_1 > T_{cool}$ (i.e., $\xi_{cool} > \xi_2$), which is the situation in Fig. 12. Then the time spent waiting at T_1 will have no effect on the behavior at T_2 because this will only change correlations at scales larger than ξ_2 that are anyway frozen at T_2. The important correlations are those of scales between ξ_{min} and ξ_2 and these only freeze out during the subsequent cooling from T_{cool} to T_2; see Fig. 12. Provided correlations on length scales between ξ_{min} and ξ_2 depend on temperature [through the temperature dependence of the exponent $\alpha(T)$ in Eq. (20)], these will have to reequilibrate while waiting at T_2, and so there will be a rejuvenation signal. Furthermore, the signal will be same for the direct quench and the temperature shift from T_1, i.e. we have full rejuvenation.

On the other hand, if $T_1 < T_{cool}$ (so $\xi_{cool} < \xi_2$) waiting at T_1 does enhance correlations at scales $\lesssim \xi_2$ (to be precise, at scales between ξ_{cool} and ξ_2) relative to a direct quench. Hence rejuvenation will only be partial in this case.
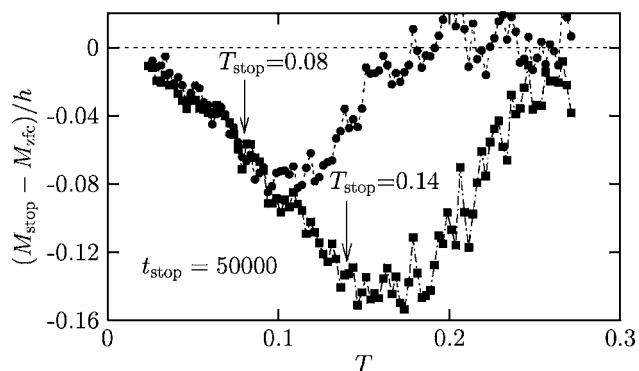

FIG. 13. Effect of a stop during cooling on the zero-field cooled magnetization. The duration of the stop is $t_{stop} = 5 \times 10^4$, and two temperatures $T_{stop} = 0.14$ (squares) and $T_{stop} = 0.08$ (circles) are used, as shown by vertical arrows. We plot the difference between M_{stop} and M_{zfc}, the zero-field cooled magnetizations with and without the stop, respectively. The cooling and heating rates are $R = 5 \times 10^{-6}$, the magnetic field is $h = 0.01$. A dip centered around T_{stop} is observed, but this is broader than in experiments.

Hence we can succinctly express the condition for full rejuvenation as

$$\xi_{cool} > \xi_2 \quad \text{(full rejuvenation)}, \qquad (31)$$

or in other words, the correlation length developed at $T = T_1$ during cooling is greater than the correlation length subsequently developed during waiting at the lower temperature $T = T_2$.

To get a rough idea of the numbers implicit in Eq. (31), we take the simple barrier activation model for $\xi(T, t)$ discussed in Sec. II in which $\xi(T, t)$ is assumed to be a function of $T \ln t$. The condition for full rejuvenation, Eq. (31), then becomes

$$\frac{T_1 - T_2}{T_2} > \frac{\ln(t_2/t_{cool})}{\ln t_{cool}} \quad \text{(full rejuvenation)}. \qquad (32)$$

The deviations from simple barrier activation used in the plots in Fig. 12 actually allow full rejuvenation when T_1 is somewhat closer to T_2 than given by Eq. (32). Since we need $t_2 \gg t_{cool}$ (otherwise the signal is dominated by initial transients), Eq. (32) implies that t_2 must be huge.

Given our numerical results[1] for $\xi(T, t)$, we estimate that $t_{cool} > 10^3$ is at least necessary to satisfy Eq. (31), implying that the total cooling time is about 10^5, so that aging times should be $t_1 \sim t_2 \gg 10^5$ that is not presently feasible in simulations. This justifies our inability to reach the full rejuvenation limit in this numerical work, as opposed to experimental investigations. By contrast, perfect memory effects can be obtained in simulations because they do not rely on the existence of finite cooling rates; compare Eqs. (18) and (32).

We also suspect that Eq. (32) is necessary to observe the spectacular "dip" in ac susceptibility measurements.[11] The reason a sharp dip has not been seen in simulations[31] is, in our view, because the times scales did not satisfy Eq. (32). In an effort to get closer to Eq. (32), we have reproduced the experimental protocol of Ref. 15, where a dip experiment is realized using the magnetization as a physical observable.

The system is gradually cooled at rate $R=5\times10^{-6}$ from high temperature, $T_i=0.35$, to very low temperature $T=0.02$. It is then immediately reheated at the same rate R with a small magnetic field, $h=0.01$, which ensures a linear response.[54] The zero field cooled magnetization, $M_{zfc}(T)$, is then recorded. We then repeat the same protocol but this time include a stop of duration t_{stop} at temperature T_{stop} during cooling. Upon reheating we now measure $M_{stop}(T)$. The difference $M_{stop}-M_{zfc}$ for $t_{stop}=5\times10^4$ and two different temperatures, $T_{stop}=0.14$ and $T_{stop}=0.08$ is presented in Fig. 13. Curves have the typical shape found in experiments[15] where the difference is maximal close to T_{stop} and becomes 0 at smaller and larger temperatures. However, the dip found here is broader than in experiments. The fact that the curve has a bump at T_{stop} is akin to a memory effect since upon reheating the system remembers it has aged there. The fact that the difference diminishes at $T<T_{stop}$ is a rejuvenation effect, because despite having aged close to T_{stop} the magnetization gets close to the reference curve. A full rejuvenation would imply that the difference really goes to 0. As above, we do find a good amount of memory but only a partial rejuvenation, because the separation of time scales is smaller than in experiments.

Recently, experiments have been carried out on superspin glasses,[12] in which the microscopic time scale t_0 is considerably larger than in standard spin glasses ($t_0\simeq10^{-5}$ s), and so the time scales probed are closer to those of our simulations than in experiments on standard spin glasses. Interestingly, results of these experiments are quite similar to those of our simulations and, in particular, rejuvenation is only partial, even when temperature steps are quite substantial. In our view, the claim made in Ref. 12 that rejuvenation is "absent" is merely a matter of definition, and we prefer to say that rejuvenation exists but is not full. The lack of full rejuvenation observed in superspin glasses is consistent with our discussion if the spread of time scales is not large enough for Eq. (31) and (32) to be satisfied. Implicit in Ref. 12 is the idea that full rejuvenation necessarily implies strong temperature chaos. However, we have argued here that full rejuvenation does not require temperature chaos; just a large separation of time scales and a temperature shift that is not too small.

VI. SUMMARY

We have numerically studied memory and rejuvenation effects in the three-dimensional Heisenberg Edwards-Anderson spin glass. The main difference between experiments and simulations is that the simulations have a much less pronounced separation of time scales. As a result, memory effects in temperature cycles can only be observed numerically for larger temperature shifts than in experiments.

Similarly, we find that the time scale gap between experiments and simulations also produces a qualitative difference when Ising and Heisenberg models are compared. In our numerical time window, the effect of a temperature shift on aging dynamics is stronger for Ising systems than for Heisenberg systems, see Fig. 10 and Sec. IV C, since the dynamic correlation length varies more strongly with T in the Ising case. However, in experiments, the effect is the opposite.[8,14] The numerical data shift, but only slowly, toward experimental observations when larger time scales are simulated; see Fig. 11.

In addition to memory effects, we also observe partial rejuvenation for large temperature shifts. However, we find no sign of temperature chaos, even for much larger temperature shifts than in the experiment. The main difference between the results of simulations, including ours and experiments is that simulations never find full rejuvenation. We have given an explanation of this which does not involve temperature chaos but rather depends on (i) the finite cooling rate in experiments and (ii) the much larger separation of time scales in experiments than in simulations. The finite cooling rate also appears to be the explanation for the "sub-aging" behavior found in experiments.

ACKNOWLEDGMENTS

*Electronic address: berthier@lcvn.univ-montp2.fr; URL: http://w3.lcvn.univ-montp2.fr/~berthier

†Electronic address: peter@bartok.ucsc.edu; URL: http://bartok.ucsc.edu/peter

[1] L. Berthier and A. P. Young, Phys. Rev. B **69**, 184423 (2004).

[2] E. Vincent, J. Hamman, M. Ocio, J.-P. Bouchaud, and L. F. Cugliandolo, in *Complex Behavior of Glassy Systems*, edited by M. Rubi (Springer-Verlag, Berlin, 1997).

[3] P. Nordblad and P. Svendlidh, in *Spin Glasses and Random Fields*, edited by A. P. Young (World Scientific, Singapore, 1998).

[4] L. Berthier, V. Viasnoff, O. White, V. Orlyanchik, and F. Krzakala, in *Slow Relaxation and Non-Equilibrium Dynamics in Condensed Matter*, edited by J.-L. Barrat, J. Dalibard, M.

Feigelman, and J. Kurchan (Springer-Verlag, Berlin, 2003).

[5] V. Dupuis, E. Vincent, J.-P. Bouchaud, J. Hammann, A. Ito, and H. A. Katori, Phys. Rev. B **64**, 174204 (2001).

[6] P. E. Jönsson, H. Yoshino, and P. Nordblad, Phys. Rev. Lett. **89**, 097201 (2002).

[7] P. E. Jönsson, R. Mathieu, P. Nordblad, H. Yoshino, H. A. Katori, and A. Ito, Phys. Rev. B **70**, 174402 (2004).

[8] F. Bert, V. Dupuis, E. Vincent, J. Hammann, and J.-P. Bouchaud, Phys. Rev. Lett. **92**, 167203 (2004).

[9] P. Réfrégier, E. Vincent, J. Hammann, and M. Ocio, J. Phys. (France) **48**, 1533 (1987).

[10] J. Hammann, M. Lederman, M. Ocio, R. Orbach, and E. Vincent, Physica A **185**, 278 (1992).

[11] K. Jonason, E. Vincent, J. Hammann, J.-P. Bouchaud, and P. Nor-

dblad, Phys. Rev. Lett. **81**, 3243 (1998).

[12] P. E. Jönsson, H. Yoshino, H. Mamiya, and H. Takayama, cond-mat/0405276.

[13] M. Sasaki, V. Dupuis, J.-P. Bouchaud, and E. Vincent, Eur. Phys. J. B **29**, 469 (2002).

[14] V. Dupuis, F. Bert, J.-P. Bouchaud, J. Hammann, F. Ladieu, D. Parker, and E. Vincent, cond-mat/0406721.

[15] R. Matthieu, P Jönsson, D. N. H. Nam, and P. Nordblad, Phys. Rev. B **63**, 092401 (2001).

[16] L. C. E. Struik, *Physical Aging in Amorphous Polymers and Other Materials* (Elsevier, Houston, 1978).

[17] A. S. Wills, V. Dupuis, E. Vincent, J. Hammann, and R. Calemczuk, Phys. Rev. B **62**, R9264 (2000).

[18] R. L. Leheny and S. R. Nagel, Phys. Rev. B **57**, 5154 (1998).

[19] H. Yardimci and R. L. Leheny, Europhys. Lett. **62**, 203 (2003).

[20] A. V. Kityk, M. C. Rheinstädter, K. Knorr, and H. Rieger, Phys. Rev. B **65**, 144415 (2002).

[21] F. Alberici-Kious, J.-P. Bouchaud, L. F. Cugliandolo, P. Doussineau, and A. Levelut, Phys. Rev. Lett. **81**, 4987 (1998).

[22] L. Bellon, S. Ciliberto, and C. Laroche, Eur. Phys. J. B **25**, 223 (2002).

[23] E. V. Colla, L. K. Chao, and M. B. Weissman, Phys. Rev. B **63**, 134107 (2001).

[24] O. Kircher and R. Böhmer, Eur. Phys. J. B **26**, 329 (2002).

[25] A. Vaknin, Z. Ovadyahu, and M. Pollak, Phys. Rev. B **65**, 134208 (2002).

[26] H. Rieger, J. Phys. I **4**, 883 (1994).

[27] J. Kisker, L. Santen, M. Schreckenberg, and H. Rieger, Phys. Rev. B **53**, 6418 (1996).

[28] T. Komori, H. Yoshino, and H. Takayama, J. Phys. Soc. Jpn. **69**, 1192 (2000).

[29] L. Berthier and J.-P. Bouchaud, Phys. Rev. B **66**, 054404 (2002).

[30] L. Berthier and J.-P. Bouchaud, Phys. Rev. Lett. **90**, 059701 (2003).

[31] M. Picco, F. Ricci-Tersenghi, and F. Ritort, Phys. Rev. B **63**, 174412 (2001).

[32] A. Maiorano, E. Marinari, and F. Ricci-Tersenghi, preprint cond-mat/0409577.

[33] S. Jimenez, V. Martin-Mayor, and S. Perez-Gaviro, preprint cond-mat/0406345.

[34] D. S. Fisher and D. A. Huse, Phys. Rev. Lett. **56**, 1601 (1986); Phys. Rev. B **38**, 373 (1988); Phys. Rev. B **38**, 386 (1988).

[35] L. F. Cugliandolo and J. Kurchan, Phys. Rev. B **60**, 922 (1999).

[36] J.-P. Bouchaud, in *Soft and Fragile Matter: Non Equilibrium Dynamics, Metastability and Flow*, edited by M. E. Cates, and M. R. Evans (Institute of Physics Publishing, Bristol, 2000).

[37] J.-P. Bouchaud, V. Dupuis, J. Hammann, and E. Vincent, Phys. Rev. B **65**, 024439 (2001).

[38] H. Yoshino, A. Lemaître, and J.-P. Bouchaud, Eur. Phys. J. B **20**, 367 (2001).

[39] L. Berthier and P. C. W. Holdsworth, Europhys. Lett. **58**, 35 (2002).

[40] F. Scheffler, H. Yoshino, and P. Maas, Phys. Rev. B **68**, 060404 (2003).

[41] M. Sasaki and O. C. Martin, Phys. Rev. Lett. **91**, 097201 (2003).

[42] H. Yoshino, J. Phys. A **36**, 10819 (2003).

[43] H. Kawamura, Phys. Rev. Lett. **80**, 5421 (1998); **90**, 237201 (2003).

[44] L. Berthier and A. P. Young, J. Phys.: Condens. Matter **16**, S729 (2004).

[45] H. Takayama and K. Hukushima, J. Phys. Soc. Jpn. **73**, 2077 (2004).

[46] V. S. Zotev, G. F. Rodriguez, G. G. Kenning, R. Orbach, E. Vincent, and J. Hammann, Phys. Rev. B **67**, 184422 (2003).

[47] A. J. Bray and M. A. Moore, Phys. Rev. Lett. **58**, 57 (1987).

[48] T. Aspelmeier, A. J. Bray, and M. A. Moore, Phys. Rev. Lett. **89**, 197202 (2002).

[49] M. Sasaki, K. Hukushima, H. Yoshino, H. Takayama, preprint cond-mat/0411138.

[50] F. Krzakala, Europhys. Lett. **66**, 847 (2004).

[51] L. Berthier, P. C. W. Holdsworth, and M. Sellitto, J. Phys. A **34**, 1805 (2001).

[52] See http://www.sheilaomalley.com/archives/002514.html

[53] H. Yoshino and P. E. Jönsson, preprint cond-mat/0407459.

[54] L. Berthier and A. P. Young (unpublished).